

Efficient Data Representation for Motion Forecasting: A Scene-Specific Trajectory Set Approach

1st Abhishek Vivekanandan

FZI Research Center for Information Technology
Karlsruhe, Germany
vivekanandan@fzi.de

2nd J. Marius Zöllner

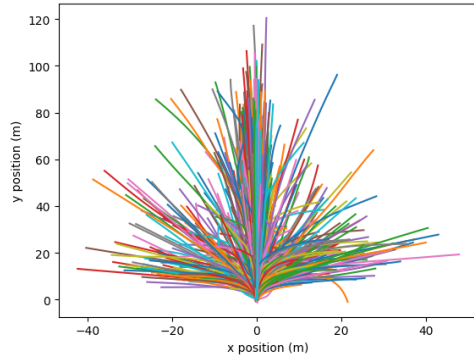
FZI Research Center for Information Technology
KIT - Karlsruhe Institute of Technology
Karlsruhe, Germany
zoellner@fzi.de

Abstract—Representing diverse and plausible future trajectories is critical for motion forecasting in autonomous driving. However, efficiently capturing these trajectories in a compact set remains challenging. This study introduces a novel approach for generating scene-specific trajectory sets tailored to different contexts, such as intersections and straight roads, by leveraging map information and actor dynamics. A deterministic goal sampling algorithm identifies relevant map regions, while our Recursive In-Distribution Subsampling (RIDS) method enhances trajectory plausibility by condensing redundant representations. Experiments on the Argoverse 2 dataset demonstrate that our method achieves up to a 10% improvement in Driving Area Compliance (DAC) compared to baseline methods while maintaining competitive displacement errors. Our work highlights the benefits of mining such scene-aware trajectory sets and how they could capture the complex and heterogeneous nature of actor behavior in real-world driving scenarios.

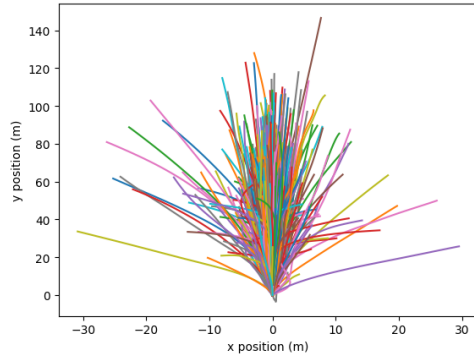
Index Terms—motion forecasting, planning, safety, trajectory sets, plausibility

I. PROLOGUE

The need for scene-specific trajectory sets arises from the inherent variability in driving environments. Different scenes—such as intersections, roundabouts, or straight roads—impose unique constraints on vehicle movement due to factors like road geometry, traffic rules, and potential interactions with other vehicles. A single set of trajectories cannot capture this diversity effectively because it lacks the contextual information needed to represent plausible behaviors across all scenarios. For example, at intersections, vehicles may turn left, right, or go straight, each requiring different trajectory predictions based on lane geometry and traffic signals. In contrast, on straight roads, fewer trajectory variations are needed because vehicles typically follow a more predictable path. By generating scene-specific trajectory sets, we can ensure that the predicted trajectories are not only diverse but also plausible within the specific context of each scene. Moreover, using a single set risks either under-representing possible outcomes (leading to unsafe predictions) or over-representing them (resulting in computational inefficiency). Scene-specific sets strike a balance by focusing computational resources on the most relevant trajectories for each scenario. This approach enhances both safety and performance in autonomous driving



(a)



(b)

Fig. 1: A Set for (a) Intersection Scenes and (b) Non-Intersection Scenes

systems by ensuring that predictions align more closely with real-world constraints and behaviors.

II. INTRODUCTION

In Autonomous Driving, motion forecasting of actors surrounding the ego vehicle has been a persistent challenge due to the evolving complexities associated with a scene, exacerbated by the inherent nature of dynamic interactions between different traffic participants. Capturing such interactions through discrete intent has been successful to some extent,

but such representations lack multi-modality to capture the true posterior distribution of the actors. Consequently, motion forecasting demands multi-modality of plausible outcomes, defining the intended actions required to reach a particular goal position [1]. The associated model uncertainty can result in system behavior that is non-conformant with both physics and scene geometry. In certain situations, this non-conformance can lead to fatal consequences. [2]

Trajectory sets play a crucial role in encoding physics into the motion forecasting layer of an autonomous driving (AD) stack, as demonstrated in the works of [3]–[5]. These sets provide a structured representation of the possible future trajectories of traffic participants sampled from the training distribution. By incorporating such trajectory sets into the motion forecasting process, the AD system can generate predictions that are more consistent with the vehicle kinematics and geometric constraints of the scene.

Existing methods compute sets independent of the underlying scene representation (acquired from HD maps) and solely rely on minimizing a cost function based on some metrics. This leads to pertinent gaps about constructing an effective set, whereby the cost function includes a geometric correlation between reachability and the implied metrics. Sets, therefore, must be carefully designed to balance the diversity of plausible outcomes; failure to achieve this balance can lead to suboptimal system behavior arising out of sparsity problems within the output representation space [5]. This is because constructing such an optimal set is a max-min k-dispersion problem, which belongs to the NP-hardness complexity [6]. Through this work, our contributions are twofolds:

- **Scene-Specific Trajectory Set Generation:** We introduce a novel algorithm for creating scene-specific trajectory sets by leveraging HD map information and actor state. Our method constructs a directed graph from the vector map, performs a depth-first search to identify goal lanes, and categorizes scenes into intersection and non-intersection bins. This approach enables the generation of tailored trajectory sets that better represent the geometric constraints and likely actor behaviors for each scene type, improving both diversity and plausibility of trajectories.

- **Empirical Analysis of Sampling Methods and Set Sizes:** Through extensive experiments on the Argoverse 2 dataset, we investigate the impact of different sampling strategies and set sizes on the diversity and plausibility of the generated trajectory sets. We conduct a comprehensive empirical study comparing metric-driven, random sampling, and our proposed Recursive In-Distribution Subsampling (RIDS) methods across various set sizes (1k to 5k trajectories). The results demonstrate that sampling from a uniform distribution using RIDS outperforms the metric-driven method in terms of retaining more plausible trajectories while maintaining comparable displacement errors. We empirically show that RIDS can effectively condense the full representation space to a manageable set size while preserving coverage and plausibility. Furthermore, our analysis reveals the optimal balance between

set size and performance metrics, providing insights for efficient trajectory set generation in downstream motion forecasting tasks.

III. RELATED WORKS

The trajectory prediction problem has been predominantly addressed using *regression* approaches, which aim to predict a set of waypoints that closely resemble the ground truth trajectory. During training, the loss between the ground truth and the model prediction is optimized. However, *regression* methods often rely on anchors to enforce diversity between trajectories and require anchors for preventing the models against mode collapse [7], [8]. Regression-based approaches without explicit integration of prior knowledge leads to predictions which go off-road [9] without respecting the neither the underlying kinematics nor the environment [5], [10].

Trajectory Sets in Planning and Prediction Trajectory sets have emerged as a choice in motion prediction, particularly in autonomous driving, as they model the uncertain future as a distribution over a compact set of possible trajectories for each agent. Predominantly, trajectory sets or trim trajectories have been used in planning [11] to resolve for a valid path at a constant time and memory. This flexibility has demonstrated state-of-the-art performance [3], [4], [12] by reformulating the problem as a *classification* where each of the trajectories in the set represents an individual anchor [8]. This effectively avoids mode collapse, which can occur with models when trained with a regression loss. While traditional methods like Bayesian approaches [13] can be computationally intensive and may pose limitations for real-world applications, whereas trajectory sets offer a practical and empirically superior alternative.

Multiple Sets for Improved Representation Single-set representations often fail to capture the true posterior distribution of ground truth probabilities in real-world scenarios due to sparsity and model expressivity issues [5], [14]. We propose using multiple subsets to create a denser representation space that better approximates ground truth probabilities and trajectory existence. The effectiveness of these sets depends on scene clustering methods, which can be supervised or semi-supervised [15]. Various approaches exist, from using traffic actors' state vectors with criticality metrics [16]–[18] to clustering based on agent trajectories [19]. Our method employs an L-norm metric between lane centerlines and the target actor's current state, avoiding the look-ahead bias present in other methods that require full actor state representation to create cluster bins.

In our previous work [5], we investigated the approach of pruning trajectory sets based on their intersection with non-drivable regions. However, the generated set lacked priors knowledge with map information, leading to a significant number of trajectories being discarded due to non-plausible states. To address this limitation and build upon the new concept of multiple sets, we propose an alternative dataset-agnostic methodology that understands map information and produces multiple sets, helping to overcome sparsity issues and maintain

an optimal balance between diversity and admissibility, as discussed by Park et al. [20].

IV. PROBLEM FORMULATION

We begin by establishing the formal notations that will be consistently utilized throughout this document. Consider a full set of trajectories captured from the training distribution as T_{full} . Our objective is to deduce a subset $T' \subset T_{full}$ that maximizes the diversity and plausibility of trajectories for a cluster of scenes M_i .

$$M = \{M_i \mid i \in \mathbb{Z}^+, 1 \leq i \leq n\} \quad (1)$$

Let M be the set of all scene clusters where M_i represents an individual cluster of scenes and i is a positive integer (denoted by \mathbb{Z}^+) with n being the total number of clusters. $|T'|$ denotes the cardinality of a set T' . A trajectory T_i of an actor a_i is represented by a sequence of states, as shown in Eq. (2), where s_i^t represents the center point location (x, y) of a_i at a time t in a Cartesian coordinate frame.

$$T_i = \left\{ \underbrace{s_i^{-t_{obs}}, s_i^{-t_{obs}+1}, s_i^{-t_{obs}+2}, \dots, s_i^0}_{\text{Past states}}, \underbrace{s_i^1, s_i^2, \dots, s_i^{t_{fut}}}_{\text{Future states}} \right\} \quad (2)$$

Here, t_{obs} represents the end of the observation window, and t_{fut} represents the end of the prediction horizon. This notation aligns with the formalism used throughout the paper, particularly focusing on the representation of trajectories as sequences of states over time.

While promoting diversity (D) among the trajectories within T' , it is important to note that coverage alone is insufficient to ensure accurate and plausible output. T' should also be realistic and plausible (P), and therefore should not contain states that are physically infeasible to reach for a given scene S in M_i . Additionally, S includes lane information that delineates the probable motion paths an actor can choose to reach a goal position. Within this work, a Focal Track (FT) is of an object type car.

$$\max_{T' \subset T_{full}} [D(T') + P(T'|M_i)] \quad (3)$$

Thus, we aim to maximize Eq. (3) where we search for a set which not only optimizes for the coverage metric but also be diverse enough to sustain the environmental constraints without getting pruned [5]; a balance between diversity and plausibility.

V. SCENE-SPECIFIC SET GENERATION

A. Algorithm

The deterministic goal sampler operates on the scene S and the heading angle θ w.r.t the Focal Track to generate a set of K goal lanes, denoted as L_{goal} . This operation can be succinctly represented by the following Eq. (4):

$$L_{goal} = f(S, \theta) \quad (4)$$

Algorithm 1 Scene-Specific Set Generation

Require: Vector-Map (m), State (s_i) Information of Focal Track FT

- 1: **for** each Scene **do**
- 2: Construct a directed graph G from m
- 3: $s_i, \theta \leftarrow$ Query for the focal track states, where θ is the heading angle
- 4: $R \leftarrow$ Calculate Rotation Matrix with θ
- 5: $N_{nearest} \leftarrow$ Filter for edges with parallel direction vectors to FT
- 6: $n_{source} \leftarrow$ Find the source node using L1-norm between s_i^0 and $N_{nearest}$
- 7: $L_{goal} \leftarrow$ Perform DFS on all the nodes in $N_{nearest}$
- 8: **for** l in L_{goal} **do**
- 9: **if** l is in an Intersection **then**
- 10: **return** Trajectory, $T_{scene} = 1$
- 11: **else**
- 12: **return** Trajectory, $T_{scene} = 0$
- 13: **end if**
- 14: **end for**
- 15: **return** None
- 16: **end for**

Given a vector map of S and the state information of FT , the algorithm constructs a directed graph G from the map. The last observation state (s_i^0) of the FT is used to find the nearest nodes by filtering for edges with parallel direction vectors to that of the FT . This helps us find for the edges which have a higher affinity to the FT 's travelling direction, mathematically given through the dot product between the two normalized vectors (thresholding it at an angle of 10°). Within this pool of filtered edges, we choose a **source node** which fulfills the property of being closer to FT ; found by calculating the L1-norm between s_i^0 and the nearest nodes.

A Depth-First Search (DFS) is performed on each of the nearest nodes to find the **goal lanes**. For each goal lane, the algorithm checks if it is in an intersection. If any one of the lanes l in L_{goal} is present in an intersection, the trajectory is returned with a scenario tag of 1; otherwise 0. This process allows for the categorization of scenes into two bins based on the presence of goal lanes in an intersection. Running Algorithm 1 across the training dataset yields two clustered sets that reflect the local representation of the scene, as shown in Fig. 1a and Fig. 1b. The trajectories corresponding to the scenes are normalized to FT 's last observation state using the rotation matrix R .

As we will see in the upcoming chapters, how this clustering maximizes the probability of finding trajectories closer to the ground truth without compromising on the shortcomings of earlier approaches which utilize a single set. To optimize the clustered sets further, we need to determine two key parameters: *the optimal set size* and *the sampling strategy*. The sampling approach plays a crucial role in reducing the clustered sets to an optimal size suitable for the intended application.

VI. METRICS

The distance between trajectories within a set is quantified using Euclidean metrics, such as the minimum Average Displacement Error (minADE) and the minimum Final Displacement Error (minFDE). A diverse set of trajectories serves as a representative sample of the underlying population, capturing its intrinsic characteristics. By assessing the properties of each trajectory within the set, we can quantify its individual contribution to the overall diversity. To measure the plausibility of the set with respect to the drivable regions of a scene, we employ the Driving Area Compliance (DAC) score, which measures the compatibility of a set for a given scene. Therefore,

$$DAC = \frac{|T'| - n}{|T'|}$$

where, $|T'|$ represents the given set size and n denotes the number of non-compliant trajectories which goes off-road. A higher DAC score provides an indication of the set's density in relation to the scene. We use the same methodology as described in [5] to get the DAC value per scene. By integrating the DAC and Euclidean metrics, we enhance our assessment of the set's quality, which hinges on its closeness to the ground truth trajectories. A higher DAC score signifies that more trajectories adhere to drivable areas, whereas lower minADE values indicate closer alignment with the ground truth. Employing both diversity and scene compliance metrics ensures that the optimized set of trajectories maximizes the representativeness of the set, providing a comprehensive portrayal of the true population dynamics w.r.t the map geometry.

To evaluate the quality of our constructed trajectory set, we establish a theoretical Lower Bound (LB) through comparison with the T_{full} which provides us with the required query trajectories¹. The LB computation process operates as follows: for each query trajectory $q \in T_{full}$, we determine the closest matching trajectory T^* for a given T' by calculating minADE, formally expressed as:

$$T^* = \arg \min_{q \in T_{full}} \text{ADE}(q, T') \quad (5)$$

The LB is then computed as the mean of these minimum displacement errors across all query trajectories:

$$\text{LB.minADE} = \frac{1}{|T_{full}|} \sum_{q \in T_{full}} \min_{T \in T'} \text{ADE}(q, T) \quad (6)$$

This metric provides a quantitative measure of how well our constructed set captures the diversity and representativeness of the full trajectory distribution; with lower values indicating better coverage of the possible motion patterns. The *LB.minADE w/T_{full}* is an important measure for which the q originates from their respective scene types (intersection or non-intersection), thereby representing ground truth (GT) samples from the scene-specific cluster. The constructed set, however,

¹We use both query trajectory and ground truth trajectory interchangeably throughout this paper

TABLE I: Comparison of coverage-based approach vs. random sampling from the training distribution. (\downarrow) indicates lower is better, while the inverse holds true to (\uparrow). The notation $0.2m$ with Ran-Samp represents the distance threshold applied when calculating metrics for randomly sampled trajectories

Method	Set Size	LB. minADE (\downarrow)	DAC(\uparrow)
Metric Driven	1k	0.633	0.525
	1.5k	0.587	0.520
	2k	0.558	0.499
	2.5k	0.525	0.494
	3k	0.511	0.490
	4k	0.482	0.481
Ran-Samp (0.2m)	5k	0.451	0.486
	1k (854)	0.771 (0.782)	0.611 (0.673)
	1.5k (1246)	0.710 (0.737)	0.627 (0.662)
	2k (1642)	0.661 (0.667)	0.607 (0.664)
	2.5k (2067)	0.617 (0.621)	0.615 (0.678)
	3k (2450)	0.598 (0.603)	0.608 (0.682)
	4k (3237)	0.559 (0.564)	0.606 (0.671)
	5k (4023)	0.532 (0.538)	0.634 (0.675)

draws trajectories from T_{full} , enabling a comprehensive cross-evaluation of the set's performance across different scenarios.

$$Q_s \subset M_i, \quad T' \subset T_{full} \quad (7)$$

where Q_s represents the query trajectories from a specific scene type s . The establishment of this baseline metric is crucial, as it supports our hypothesis that trajectory sets sampled from T_{full} will inherently exhibit higher displacement errors compared to scene-specific sets. This phenomenon can be attributed to the inherent diversity and potential noise in the full distribution, whereas scene-specific sets benefit from more focused and contextually relevant trajectory patterns.

VII. EXPERIMENTS

We use the motion forecasting dataset from Argoverse 2 (AV2) [21], which contains 199,489 training samples or scenes and 20,000 validation samples. The construction and analysis of the validation samples are refrained from, as that would lead to look-ahead bias. Therefore, all the analysis is performed on the training distribution unless explicitly stated otherwise.

The dataset contains HD maps as a lane graph, from which we construct a directed Graph similar to VectorNet polyline [22] representation. Every scene has a target actor called as a focal track (FT), whose observation window satisfies the requirement of possessing full state information throughout the complete sampling horizon. For AV2, the sampling horizon is 6s for the future, with a 5s observation history; sampled at 10Hz. A Rotation matrix R is calculated using the heading angle and the last XY coordinate at a time step t_{obs} . The trajectory T_i is transformed into a local coordinate system (actor-centric) by applying R , which is better suited to represent trajectories.

A. Evaluation of sets on T_{full}

Validating the effectiveness of the sets is crucial to comprehend the influence of two primary parameters which govern

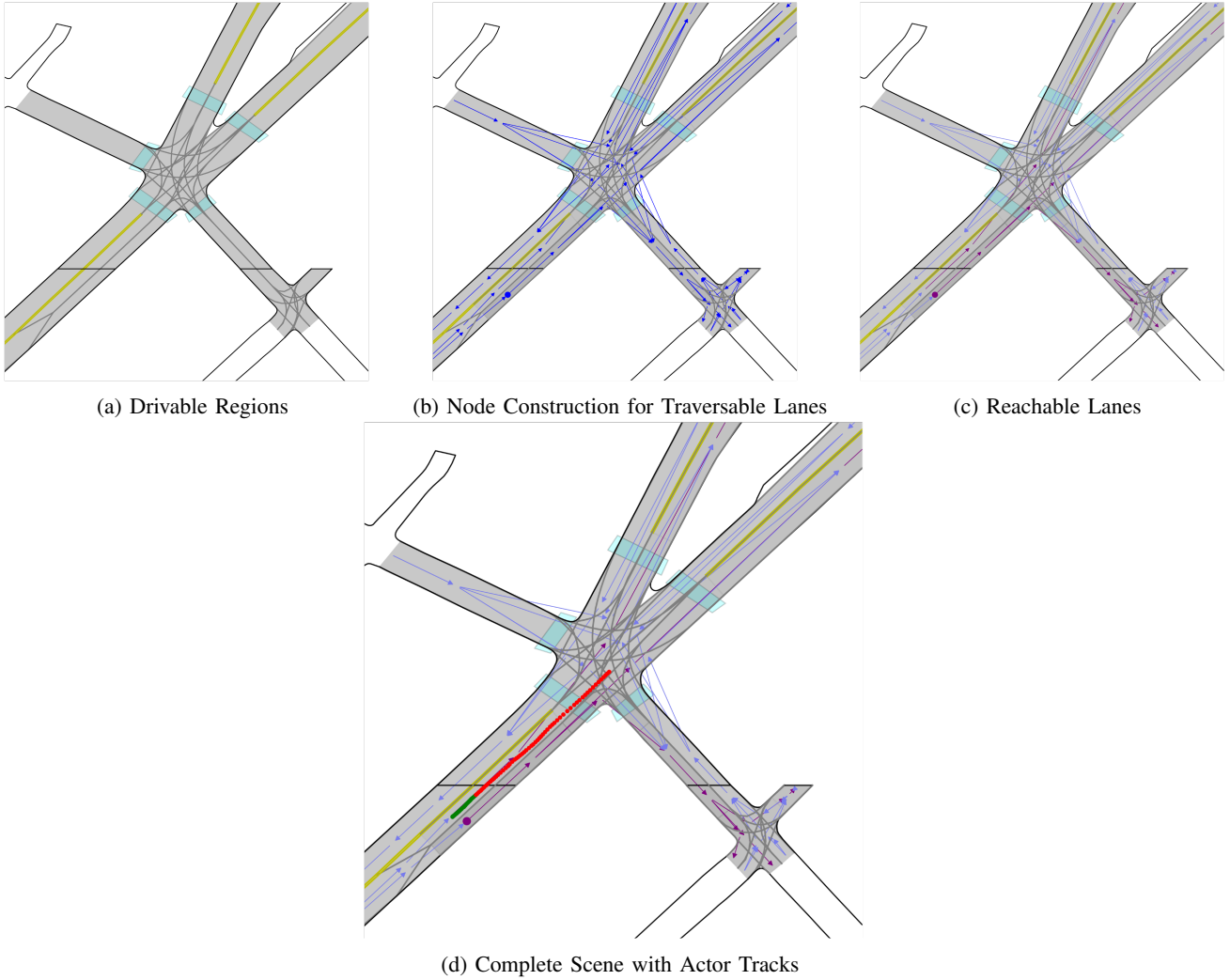


Fig. 2: Steps involved in clustering the scenes based on the road geometry and actor states are shown here. **Past trajectory** and **Future trajectory** of an FT are illustrated. In (a), Grey connections denote the connectivity between various lanes at an intersection. In (b), **Blue edges** depict the transformation of lane connections into node edges. Using Algorithm 1, the **Source node**, which corresponds to the closest node relative to the last observed state of the FT, is identified. Finally, the edges in (c) represent the plausible lanes the FT could potentially select.

diversity and plausibility. We employ the *metric-driven* method [12] and a random sampling to demonstrate the efficacy of our proposed scene-specific set generation concept. Similar to the Covernet [3]; *metric-driven* method also employs a minADE driven bagging algorithm to reduce each of the clustered sets, we have acquired from the Algorithm 1. Random sampling (*Ran-Samp*) is used as a baseline, and we report the lowest value as it exhibits a variance of $\pm 2\%$. By comparing the performance of our method against the baseline and analyzing the lower bounds, we gain insights into how effective our set construction is in capturing diverse and plausible trajectories.

Table I illustrates the effect of *metric-driven* sets when compared with randomly sampled sets generated from the training distribution. As the set size increases, the LB of the metrics linearly decreases, this is attributed to the presence of more trajectories which lie closer to a given q , thereby

providing good coverage. Sets generated through the *metric-driven* method perform well as expected, since the cost function enforces diversity between the trajectories in the set when compared with *Ran-Samp*. On the other hand, from Fig. 3 emerges a wholly different picture. The normalized rate of surviving trajectories, that which are compliant with the scene, is substantially higher for the *Ran-Samp* and amounts to 10% more trajectories irrespective of the set size.

The *Ran-Samp* method, however, is not without its drawbacks. It includes trajectories that overlap and are deemed redundant, which could be eliminated without adversely affecting the metrics. To address this, we introduce a thresholding rate of 0.2m, enabling the removal of redundant trajectories that lie close to each other within the *Ran-Samp* set. This refinement process results in a more lean set, reducing the number of trajectories by approximately 15% compared to the original set size, as

can be seen from Table I. Moreover, this process improves the DAC rate while preserving an equivalent minADE when juxtaposed with simple *Ran-Samp* set.

B. Evaluation of scene-specific sets

Utilizing Algorithm 1, we generate two distinct clustered sets: one pertaining to intersections and the other to non-intersections. Subsequently, for each clustered set, adhering to their corresponding sampling criteria, we performed extensive analysis, as can be seen from the Table II.

The *LB.minADE* column of Table II, when evaluated against the results from the Table I shows similar correlation between the internal representation of trajectories (sets' diversity) and the set size. As we incrementally increase the set size from 1k to 5k, the *LB.minADE* shows a consistent decrease for both methods (*metric-driven* and *Ran-Samp*) and across both scenario types (Non-intersection and intersection set). This suggests that the generation of scene-specific sets increases the probability of finding more trajectories that lie closer to the ground truth.

The *DAC* metric exhibits relative stability across different set sizes for each method and scenario combination. The *Ran-Samp* method consistently shows higher *DAC* values compared to *metric-driven*, suggesting that it is more effective in generating a set where a larger proportion of the trajectories remain plausible. When comparing the two scenario types, it is evident that both methods yield poorer performance in intersection scenarios compared to non-intersections, as measured between corresponding *LB.minADE* metrics. This outcome is anticipated due to the increased complexity and diversity of potential trajectories at intersections. However, the performance degradation from non-intersection to intersection scenarios is less evident for *Ran-Samp* than for *metric-driven*. As set sizes increase, the displacement error narrows, and the number of surviving trajectories experiences a significant increase, a trend that is also observable in the intersection sets.

We also created a new subsampling algorithm, *RIDS* or *Recursive In-Distribution Subsampling*, where we remove overlapping trajectories from a set constructed using *Ran-samp*. If two trajectories share proximity to each other and lie within a threshold of $0.2m$ to each other, we consider this trajectory redundant and arbitrarily remove one of them. This leaves us with a set which is underweighted; to counter this, we perform subsampling from the training distribution and recursively perform this step of removing and adding trajectories until the desired T' is reached.

VIII. RESULTS AND DISCUSSIONS

The ultimate goal of this work is to find the answer to the following question: *What is the best conceptual framework that can maximize the probability of finding trajectories closer to the ground truth?* This led us to investigate and propose a scene-specific set generation method, which, when viewed through the lenses of displacement errors and *DAC*, gives better performance compared to an uninformed set. The next step is to find the sampling method; From Fig. 3, random

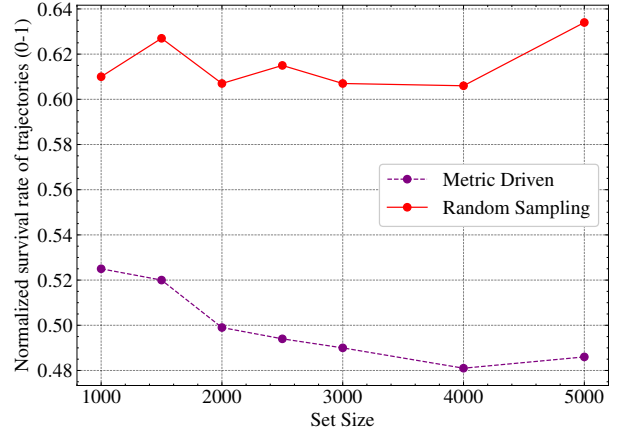


Fig. 3: The randomly sampled sets can retain more number of trajectories when compared with a metric-driven set, making the former a reliable way to represent more plausible states

sampling provides preliminary evidence, as it retains more trajectories than *metric-driven* when one wants to achieve a dense representation of the set.

Trajectory sets are used for the downstream task of motion prediction of actors in the environment, where the probability of finding more trajectories outweighs the minimal performance gains from the displacement metrics. In this case, a set that maximizes plausibility is desired if the nominal gains from the Euclidean metrics are minimal, since we can guarantee that there exist more trajectories in the proximity which can represent the ground truth.

Although the *metric-driven* method was able to provide guarantees of probabilistic completeness to maximize coverage, it did not capture the true distribution, providing insufficient exploration. On the other hand, sampling from a uniform distribution; *RIDS* was able to retain more trajectories and outperform the *metric-driven* method. The property of an efficient estimator is that it has the smallest possible variance, indicating that it is closest to the true value of the parameter being estimated. This reasoning that *RIDS* being an efficient estimator and functions effectively because in certain optimization situations, sampling from the underlying distribution can be more efficient than performing sampling based on some metrics.

Our experiments have shown that the scene-specific set generation method allows us to improve diversity, and more specifically, *RIDS*; a variant of random sampling works relatively well when considering the environment, resulting in an improved *DAC* score. The survival rate for the trajectories for sets constructed using *Ran-Samp* and *RIDS* outperforms *metric-driven* methods, given that the minimal gain in displacement errors from *metric-driven* overshadows the presence of more plausible trajectories. A visual distinction is notable for the non-intersection set in Fig. 1a, which confirms our prior, as most of the trajectories do not represent significant yaw differences (going straight). The *DAC* score for the non-intersection with *Ran-Samp* depicts that cluster-based trajec-

TABLE II: Quantitative comparison of Scene-specific sets with different methods on Argoverse 2 training distribution

Method	Set Size	Non-Intersection Set			Intersection Set		
		LB. minADE (\downarrow)	LB. minADE w/ T_{full} (\downarrow)	DAC(\uparrow)	LB. minADE (\downarrow)	LB. minADE w/ T_{full} (\downarrow)	DAC(\uparrow)
Metric Driven	1k	0.592	0.670	0.694	0.722	0.735	0.518
	1.5k	0.531	0.628	0.673	0.667	0.672	0.500
	2k	0.500	0.593	0.677	0.621	0.639	0.490
	2.5k	0.472	0.567	0.664	0.599	0.608	0.484
	3k	0.443	0.544	0.704	0.575	0.585	0.477
	4k	0.416	0.527	0.692	0.547	0.553	0.468
	5k	0.388	0.491	0.687	0.510	0.528	0.469
Ran-Samp	1k	0.727	0.830	0.827	0.874	0.892	0.691
	1.5k	0.673	0.748	0.831	0.789	0.813	0.664
	2k	0.601	0.685	0.823	0.729	0.746	0.663
	2.5k	0.568	0.654	0.842	0.690	0.709	0.678
	3k	0.549	0.630	0.833	0.659	0.688	0.692
	4k	0.498	0.597	0.835	0.606	0.624	0.681
	5k	0.453	0.552	0.863	0.579	0.587	0.679
RIDS	1k	0.712	—	0.824	0.866	—	0.689
	1.5k	0.661	—	0.827	0.779	—	0.658
	2k	0.591	—	0.826	0.717	—	0.656
	2.5k	0.557	—	0.836	0.676	—	0.650
	3k	0.532	—	0.829	0.651	—	0.682
	4k	0.488	—	0.839	0.598	—	0.688
	5k	0.455	—	0.850	0.572	—	0.681

tory sampling works better than expected, since it can retain 86% of the trajectories for T_{5k} . This high score indicates that the set can handle the complex geometry of the real-world and is perfectly suited for the intended application. As we said at the start, this showcases that Scene-Specific Set generation can produce sets which can be tuned to represent the ground truth closer to real-world scenes than using a single set to represent diverse situations. Looking at *Ran-Samp* set created with a threshold rate of 0.2 from Table II; almost one could say that this imbalance between the set size is the reason for the improved DAC value. To counteract this argument, we performed ablation studies as can be seen from Table III and Table IV to confirm that these improved DAC values remain improved when performing the RIDS sampling process for different threshold values.

IX. CONCLUSION

In this work, we presented our approach to create scene specific set generation which retains more trajectories akin to the environment which aims to maximize for the plausibility of trajectories for a diverse amount of environment. Along with that, we also showcased that RIDS as a sampling process is effective in condensing the full representation space to a more manageable set while providing coverage and plausibility to the corresponding set.

ACKNOWLEDGMENT

The research leading to these results was funded by the German Federal Ministry for Economic Affairs and Climate Action and was partially conducted in the project “KI Wissen”. We would also like to thank Max Zipfl and Ahmed Abouelazm for their valuable reviews. Responsibility for the information

and views set out in this publication lies entirely with the authors.

REFERENCES

- [1] H. Zhao, J. Gao, T. Lan, C. Sun, B. Sapp, B. Varadarajan, Y. Shen, Y. Shen, Y. Chai, C. Schmid, C. Li, and D. Anguelov, “TNT: Target-driven Trajectory Prediction,” in *Proceedings of the 2020 Conference on Robot Learning*. PMLR, Oct. 2021, pp. 895–904, iSSN: 2640-3498. [Online]. Available: <https://proceedings.mlr.press/v155/zhao21b.html>
- [2] “Unacceptably Risky - Part 1 - Safety Report on Cruise’s Crash,” Nov. 2022. [Online]. Available: <https://www.retrospectav.com/blog/unacceptably-risky-part-1-safety-report-on-cruises-crash>
- [3] T. Phan-Minh, E. C. Grigore, F. A. Boulton, O. Beijbom, and E. M. Wolff, “CoverNet: Multimodal Behavior Prediction using Trajectory Sets,” Apr. 2020, arXiv:1911.10298 [cs, stat]. [Online]. Available: <http://arxiv.org/abs/1911.10298>
- [4] Y. Biktairov, M. Stebelyev, I. Rudenko, O. Shliazhko, and B. Yangel, “PRANK: motion Prediction based on RANKing,” in *Advances in Neural Information Processing Systems*, vol. 33. Curran Associates, Inc., 2020, pp. 2553–2563. [Online]. Available: https://proceedings.neurips.cc/paper_files/paper/2020/hash/1b0251ccb8bd5f9ccf444e4bda7713e3-Abstract.html
- [5] A. Vivekanandan, A. Abouelazm, P. Schörner, and J. M. Zöllner, “KI-PMF: Knowledge Integrated Plausible Motion Forecasting,” Oct. 2023, arXiv:2310.12007 [cs]. [Online]. Available: <http://arxiv.org/abs/2310.12007>
- [6] C. J. Green and A. Kelly, “Toward Optimal Sampling in the Space of Paths,” in *Robotics Research*, B. Siciliano, O. Khatib, F. Groen, M. Kaneko, and Y. Nakamura, Eds. Berlin, Heidelberg: Springer Berlin Heidelberg, 2010, vol. 66, pp. 281–292, series Title: Springer Tracts in Advanced Robotics. [Online]. Available: http://link.springer.com/10.1007/978-3-642-14743-2_24
- [7] H. Cui, V. Radosavljevic, F.-C. Chou, T.-H. Lin, T. Nguyen, T.-K. Huang, J. Schneider, and N. Djuric, “Multimodal Trajectory Predictions for Autonomous Driving using Deep Convolutional Networks,” in *2019 International Conference on Robotics and Automation (ICRA)*. Montreal, QC, Canada: IEEE, May 2019, pp. 2090–2096. [Online]. Available: <https://ieeexplore.ieee.org/document/8793868/>

TABLE III: Ran-Samp @ threshold of 0.5

Set size	After Threshold	Thresholded Set's LB. minADE (↓)	LB. minADE w/ T_{full} (↓)	DAC (↑)	RIDS (LB. minADE) (↓)	RIDS (DAC) (↑)
1k	713	0.807	0.780	0.645	0.747	0.641
1.5k	993	0.770	0.710	0.623	0.694	0.619
2k	1268	0.704	0.661	0.608	0.615	0.617
2.5k	1496	0.659	0.617	0.616	0.585	0.600
3k	1684	0.647	0.598	0.608	0.564	0.591
4k	2204	0.622	0.559	0.590	0.526	0.576
5k	2645	0.597	0.532	0.582	0.497	0.562

TABLE IV: Ran-Samp @ threshold of 0.2

Set size	After Threshold	Thresholded Set's LB. minADE (↓)	LB. minADE w/ T_{full} (↓)	DAC (↑)	RIDS (LB. minADE) (↓)	RIDS (DAC) (↑)
1k	854	0.782	0.780	0.673	0.752	0.676
1.5k	1246	0.737	0.710	0.662	0.712	0.662
2k	1642	0.666	0.661	0.664	0.635	0.680
2.5k	2067	0.621	0.617	0.678	0.599	0.676
3k	2450	0.603	0.598	0.682	0.572	0.671
4k	3237	0.564	0.559	0.671	0.534	0.670
5k	4023	0.538	0.532	0.675	0.503	0.663

- [8] B. Varadarajan, A. Hefny, A. Srivastava, K. S. Refaat, N. Nayakanti, A. Cornman, K. Chen, B. Douillard, C. P. Lam, D. Anguelov, and B. Sapp, "MultiPath++: Efficient Information Fusion and Trajectory Aggregation for Behavior Prediction," Dec. 2021, arXiv:2111.14973 [cs]. [Online]. Available: <http://arxiv.org/abs/2111.14973>
- [9] M. Bahari, S. Saadatnejad, A. Rahimi, M. Shaverdikondori, A. H. Shahidzadeh, S.-M. Moosavi-Dezfooli, and A. Alahi, "Vehicle trajectory prediction works, but not everywhere," in 2022 IEEE/CVF Conference on Computer Vision and Pattern Recognition (CVPR). New Orleans, LA, USA: IEEE, Jun. 2022, pp. 17102–17112. [Online]. Available: <https://ieeexplore.ieee.org/document/9878584/>
- [10] S. Casas, C. Gulino, S. Suo, and R. Urtasun, "The Importance of Prior Knowledge in Precise Multimodal Prediction," Jun. 2020, arXiv:2006.02636 [cs, stat]. [Online]. Available: <http://arxiv.org/abs/2006.02636>
- [11] M. S. Branicky, R. A. Knepper, and J. J. Kuffner, "Path and trajectory diversity: Theory and algorithms," in 2008 IEEE International Conference on Robotics and Automation. Pasadena, CA, USA: IEEE, May 2008, pp. 1359–1364. [Online]. Available: <http://ieeexplore.ieee.org/document/4543392/>
- [12] J. Schmidt, P. Huissel, J. Wiederer, J. Jordan, V. Belagiannis, and K. Dietmayer, "RESET: Revisiting Trajectory Sets for Conditional Behavior Prediction," Apr. 2023, arXiv:2304.05856 [cs]. [Online]. Available: <http://arxiv.org/abs/2304.05856>
- [13] T. A. Catnach, "Computational Methods for Bayesian Inference in Complex Systems."
- [14] C. Zhang, S. Bengio, M. Hardt, B. Recht, and O. Vinyals, "Understanding deep learning requires rethinking generalization," Feb. 2017, arXiv:1611.03530 [cs]. [Online]. Available: <http://arxiv.org/abs/1611.03530>
- [15] M. Zipf, M. Jarosch, and J. M. Zöllner, "Self Supervised Clustering of Traffic Scenes using Graph Representations," Nov. 2022, arXiv:2211.15508 [cs]. [Online]. Available: <http://arxiv.org/abs/2211.15508>
- [16] M. Zipf, B. Schütt, J. Zöllner, and E. Sax, *Fingerprint of a Traffic Scene: an Approach for a Generic and Independent Scene Assessment*, Nov. 2022.
- [17] B. Schütt, S. Otten, and E. Sax, "Clustering-based Criticality Analysis for Testing of Automated Driving Systems," Jul. 2023, arXiv:2306.12738 [cs]. [Online]. Available: <http://arxiv.org/abs/2306.12738>
- [18] L. Westhofen, C. Neurohr, T. Koopmann, M. Butz, B. Schütt, F. Utesch, B. Neurohr, C. Gutenkunst, and E. Böde, "Criticality Metrics for Automated Driving: A Review and Suitability Analysis of the State of the Art," *Archives of Computational Methods in Engineering*, vol. 30, no. 1, pp. 1–35, Jan. 2023. [Online]. Available: <https://doi.org/10.1007/s11831-022-09788-7>
- [19] J. Bernhard, M. Schutera, and E. Sax, "Optimizing test-set diversity: Trajectory clustering for scenario-based testing of automated driving systems," in 2021 IEEE International Intelligent Transportation Systems Conference (ITSC). Indianapolis, IN, USA: IEEE, Sep. 2021, pp. 1371–1378. [Online]. Available: <https://ieeexplore.ieee.org/document/9564771/>
- [20] S. H. Park, G. Lee, M. Bhat, J. Seo, M. Kang, J. Francis, A. R. Jadhav, P. P. Liang, and L.-P. Morency, "Diverse and Admissible Trajectory Forecasting through Multimodal Context Understanding," Aug. 2020, arXiv:2003.03212 [cs]. [Online]. Available: <http://arxiv.org/abs/2003.03212>
- [21] B. Wilson, W. Qi, T. Agarwal, J. Lambert, J. Singh, S. Khandelwal, B. Pan, R. Kumar, A. Hartnett, J. K. Pontes, D. Ramanan, P. Carr, and J. Hays, "Argoverse 2: Next Generation Datasets for Self-Driving Perception and Forecasting."
- [22] J. Gao, C. Sun, H. Zhao, Y. Shen, D. Anguelov, C. Li, and C. Schmid, "VectorNet: Encoding HD Maps and Agent Dynamics from Vectorized Representation," May 2020, arXiv:2005.04259 [cs, stat]. [Online]. Available: <http://arxiv.org/abs/2005.04259>